Effects of aging on low luminance contrast processing in humans

Emmanuelle Bellot, Véronique Coizet, Jan Warnking, Kenneth Knoblauch, Elena Moro, Michel Dojat

EFFECTS OF AGING ON LOW LUMINANCE CONTRAST PROCESSING IN HUMANS

Emmanuelle Bellot[a,b], Véronique Coizet[a,b], Jan Warnking[a,b], Kenneth Knoblauch[d,e], Elena Moro[a,b,c], Michel Dojat[a,b]

[a]*INSERM, U1216, F-38000 Grenoble, France*
[b]*Univ. Grenoble Alpes, Grenoble Institut des Neurosciences, GIN, F-38000 Grenoble, France*
[c]*CHU de Grenoble, Hôpital Michallon, F-38000 Grenoble, France*
[d]*INSERM U1208, Stem Cell and Brain Research Institute, F-69675 Bron, France*
[e]*Univ. Lyon 1, F-69000 Lyon, France*

emmanuelle.bellot@univ-grenoble-alpes.fr
veronique.coizet@univ-grenoble-alpes.fr
ken.knoblauch@inserm.fr
emoro@chu-grenoble.fr
jan.warnking@univ-grenoble-alpes.fr

Corresponding author:

Michel Dojat

Grenoble Institut des Neurosciences
INSERM U836
Bâtiment Edmond Safra
Chemin Fortuné Ferrini
38700 La Tronche FR

Michel.Dojat@univ-grenoble-alpes.fr

Word count: abstract = 188 words; text = 7622 words.

Short running title: Aged-related changes in superior colliculus luminance contrast processing

Abstract

Luminance contrast is a fundamental visual cue. Using a dedicated neuroimaging framework, we sought to characterize typical Blood Oxygen Level Dependent (BOLD) responses in two subcortical regions, the superior colliculus (SC) and the lateral geniculate nucleus (LGN), and V1, the primary visual cortex area, and how they change over the lifespan. For imaging subcortical activity related to luminance contrast modulation, specific measurements were introduced to rule out possible signal contamination by cardiovascular activity and vascular alterations with age that could hamper the BOLD signal interpretation. Clearly, BOLD responses increased in these three regions with luminance contrast, with a statistically significant diminution in LGN and V1 for older compared to younger participants, while basal perfusion remained unchanged. Additionally, perceptual responses, as assessed with psychophysical experiments, were highly correlated to BOLD measures in the three studied regions. Taken together, fMRI and psychophysics results indicate an alteration of luminance contrast processing with normal aging. Based on this knowledge we can better recognize when age-related brain changes vary from these expectations especially during neurodegenerative diseases progression where the functioning of subcortical structures is altered. The proposed fMRI-physchophysics methodology allows performing such investigation.

Key Words: Human Vision; Superior Colliculus; Neuroimaging; fMRI; Psychophysics.

1. Introduction

Besides cognitive impairments, visual deficits, frequently reported in normal aging, may impact daily life. Age-related visual decreases, including loss in sensitivity to motion, spatial frequency processing or luminance contrast sensitivity, are not solely due to changes in the optical properties of the eye (Elliott, Whitaker and MacVeigh, 1990; Owsley, 2011). They probably result also from age-related neuronal changes occurring along the visual pathway, at retinal (photoreceptors and ganglion cells degeneration), subcortical and cortical levels. Indeed, electrophysiological studies in animal models demonstrate that many aspects of neural and behavioral responses, such as latency (Wang, Zhou, Ma et al., 2005; Yu, Wang, Fu et al., 2005; Ball, Edwards and Ross, 2007), color discrimination (Knoblauch, Saunders, Kusuda et al., 1987; Knoblauch, Vital-Durand and Barbur, 2001), motion/speed tuning (Atchley & Andersen, 1998; Yang, Zhang, Liang et al., 2009) and contrast sensitivity (Yang, Liang, Li et al., 2008), change with aging along the multiple stages of the visual pathway. Knowledge about how in human, subcortical and cortical processing of retinal information is affected by normal aging is still missing.

Information from the retina is processed through two main pathways: the parvocellular (P) and magnocellular (M) pathways. Whereas the P pathway is responsive to chromatic and static stimulation of high spatial frequency and underlies form and chromatic discrimination along the L-M axis, the M pathway responds to achromatic stimuli with low spatial and high temporal frequencies and underlies motion and depth information processing. The majority of axons of the retinal ganglion cells (90%) that leaves the eye via the optic nerve projects to the Lateral Geniculate Nucleus (LGN), a small (5-10 mm) primary thalamic relay between the retina and the visual cortex (Sherman & Guillery, 2006). M and P pathways are mostly represented in the LGN (Felleman & Van Essen, 1991) and connected to corresponding sublayers in the primary visual area (V1). In addition to retinal afferent, LGN receives strong cortico-thalamic feedback projections from V1 (Sherman & Koch, 1986; Sherman & Guillery, 2006). This pathway is called the "*retino-geniculo-striate*" route. In parallel, a minority of fibers originating from the retina takes a secondary route and reachs the superficial layers of the Superior Colliculus (SC) (Kuypers & Lawrence, 1967; Hendrickson, Wilson and Toyne, 1970; Schiller & Malpeli, 1977). Additionnally, these layers receive inputs from the striate and extrastriate cortex (Wilson & Toyne, 1970; Benevento & Fallon, 1975; Benevento & Yoshida, 1981; Fries, 1984) and the

frontal eye field (Kuypers & Lawrence, 1967; Kunzle & Akert, 1977). There is also a projection coming from the dorsal and ventral LGN (Benevento & Fallon, 1975), especially from its M layers. In these layers visual neurons are organized in a topographical manner (DuBois & Cohen, 2000; Schneider & Kastner, 2005; Kaytal, Zughni, Greene et al., 2010) and respond to transient or moving visual stimuli (Schiller & Koerner, 1971; Cynader & Berman, 1972; Marrocco & Li, 1977). This second pathway, bypassing V1 and sending projections to extrastriate areas, is called the "*retino-tectal*" route. Compared to the well-established P pathway alteration in normal aging (Owsley, Sekuler and Siemsen, 1983; Elliott, 1987; Elliott et al., 1990; Elliott & Werner, 2010), the influence of age on the M pathway is less documented. Even if some studies suggest that there are no alterations of this pathway with aging (Owsley et al., 1983), selective loss of contrast sensitivity to relatively low spatial frequency has nonetheless been documented (Lux, Marshall, Thimm et al., 2008; Elliott & Werner, 2010; Bordaberry, Lenoble and Delord, 2012; Allard, Renaud, Molinatti et al., 2013). These controversal results about the preservation or not of the M pathway in normal aging could, in part, be due to the fact that only psychophysical data have been available. It is of interest, then, to introduce the fMRI technique for a finer non-invasive exploration of subcortical and cortical visual information processing along the M pathway and its possible alteration with age.

Advances in fMRI technique have allowed the non-invasive functional investigation of subcortical nuclei in the human brain under certain conditions (Schneider & Kastner, 2005; Sylvester, Jiosephs, Driver et al., 2007; Wall, Walker and Smith, 2009; Linzenbold, Lindig and Himmelbach, 2011). However, it remains difficult to measure the functional activity in SC (Poncelet, Wedeen, Weisskoff et al., 1992; DuBois & Cohen, 2000) because of its small size, deep location and proximity to pulsating vascular structures that may hinder the BOLD signal measurement. Moreover, SC is highly sensitive to luminance changes with a response that rapidly saturates (Schneider & Kastner, 2005) restricting the conditions of stimulation. To overcome these difficulties, we developed a low luminance contrast varying stimulus to modulate the SC activity and accordingly, a specific fMRI setting to record and analyse the corresponding BOLD signal variations in SC, LGN and V1 regions of interest. We took specific care to rule out possible signal contamination by cardiovascular activity and vascular alterations with age. We used psychophysical tests to estimate luminance contrast perception. The strong correlation we observed between perceptual and BOLD responses clearly demonstrated the validity of our

approach to non-invasively investigate the functional response of subcortical visual regions in human. We report an alteration of luminance contrast processing along the M pathway with normal aging beside the well-documented functional deficit of the P pathway. These control data and the proposed methodology allow detecting when age-related brain changes differ from these expectations in particular in neurodegenerative diseases (Rupp, Dzemidzic, Blekher et al., 2012; Rolland, Carcenac, Overton et al., 2013; Hutchinson, Isa, Molloy et al., 2014; Brace, Kraev, Rostron et al., 2015).

2. Materials and methods

2.1. Subjects

Thirty healthy subjects participated in this study. Three age-dependent groups were considered: *Young*, with 10 participants, 7 females, 26±3 years; *Middle Age*, with 10 participants, 5 females, 47±4 years and *Elderly*, with 10 participants, 7 females, 65±3 years. A visual examination by an ophthalmologist was performed for middle age and elderly participants. They had normal or corrected-to-normal vision. Participants requiring visual correction wore the MediGoggle Adult Research Set (Cambridge Research Systems Ltd, England; http://crsltd.com/), interchangeable prescriptive goggles suitable for use in MR environment. All participants provided written informed consent before participating in the study and were screened according to standard MRI exclusion criteria. The study was approved by the local ethics committee (ID-RCB 2012-A00310-43).

2.2. Psychophysical procedure

Prior to the collection of imaging data, all observers performed a Maximum Likelihood Difference Scaling (MLDS) task (Maloney & Yang, 2003; Knoblauch & Maloney, 2008; Knoblauch & Maloney, 2012) to estimate the perceived magnitude of luminance contrast changes.

2.2.1. Stimuli conditions

The stimuli (Figure 1) were composed of achromatic radial checkerboards (mean spatial frequency: 2.3 cpd, varying from 3 cpd in the center to 1.5 cpd at the periphery) with ten levels of

luminance contrast from 2 to 20%, logarithmically spaced, displayed on a neutral grey background. These stimuli were generated using Matlab (MathWorks, MA, USA). A Python homemade program was used for displaying and running the experiment, using PsychoPy2 (Peirce, 2007; Peirce, 2009) under the Windows 8 operating system. Spectral and luminance calibrations of the computer screen were performed with a PR650 SpectraScan Colorimeter (Photoresearch) and used for screen gamma-correction in stimulus specification. Stimuli had a mean luminance of 147 cd/m² equal to the grey background (CIE xy = 0.29, 0.30). Participants viewed the screen at a distance of 70 cm and the stimuli under a visual angle of 2.04°.

2.2.2. Experiment

In a dark room, each participant performed a three session experiment. Each session consisted in a 5 minute random presentation of 120 trials. On each trial, a randomly selected triad of checkerboards was presented with three luminance contrasts (a, b, c), chosen from a series of ten contrasts described above, with a < b < c. Stimulus b was always the upper stimulus in the middle, and stimuli a and c were below randomly positioned on the left or right side, respectively (see Figure 1). Stimuli were presented for 500ms. The observer was instructed to fixate the fixation cross and respond with no limit of time when he/she could choose which of the bottom patterns (left or right) was most similar to the upper pattern with respect to the luminance contrast. The observer's response initiated the next trial. The average experiment duration was 15 min. No feedback was provided to observers. After a short period of training, observers performed the task rapidly.

Insert Figure 1.

2.3. fMRI design and procedure

Subjects were presented a series of stimuli of variable luminance contrasts in each hemi-field. During the scanning run, in order to maintain and control his/her attention, the participant was instructed to fixate during the whole duration of each run the fixation cross in the center of the screen and to respond, as quickly and as accurately as possible, by pressing a button, each time the orientation of the fixation cross changed (from + to x and back to +). This task was designed in order to avoid any potential effect of unequal allocation of attention between different blocks of luminance contrast.

2.3.1. Stimuli

The stimuli were composed of achromatic radial checkerboards (mean spatial frequency: 0.42 cpd) with four levels of luminance contrast (1, 3, 5 and 9%), flashing at a frequency of 4 Hz and alternatively presented in each visual hemi-field on a grey background. Contrasts below 10% were chosen because SC response is highly sensitive to contrast with a low modulation response at higher contrast stimuli (Schneider & Kastner, 2005). Moreover, stimuli with low luminance contrast and low spatial frequency stimulate preferentially the M pathway including the SC (Derrington & Lennie, 1984; Merigan & Maunsell, 1990; Denison, Vu, Yacoub et al., 2014; Zhang, Zhou, Wen et al., 2015). Luminance contrast was defined as Michelson contrast, $\frac{L_{max}-L_{min}}{L_{max}+L_{mn}}$, where L_{max} and L_{min} were the maximum and minimum luminance in the stimuli respectively. These stimuli were generated using Matlab (MathWorks, MA, USA) and displayed with the Psychophysics toolbox extension (Brainard, 1997; Pelli, 1997) running on the same computer as that used for the psychophysical experiments. Stimuli were back-projected using a LCD video-projector projector (Epson 7250M, Epson Inc., Long Beach, CA) onto a translucent screen positioned at the rear of the magnet. Spectral and luminance calibrations of the display were performed with a PR650 SpectraScan Colorimeter (Photoresearch) and used for screen gamma-correction in stimulus specification. Stimuli had a mean luminance of 147 cd/m² equal to the grey background (CIE xy = 0.29, 0.30). Participants viewed the screen at a distance of 128 cm via a mirror fixed on the head coil and the stimuli under a visual angle of 14° horizontally and 14° vertically.

2.3.2. Experiment

We used a block-design paradigm with four luminance contrast levels (1, 3, 5 and 9%). These levels were selected to maximize the perceptual effect as assessed with the MLDS test (see Results Section). The functional session consisted of nine scanning runs, each run lasting 4 minutes and 12 seconds. Each run was composed of four main blocks of visual stimulation (see Figure 2), each being composed of four 12-second blocks (one block per luminance contrast level), plus five 12-second fixation intervals (fixation cross in the center of the screen) including one at the start, one at the end and one between each main block. The order of luminance contrast levels was randomized within blocks. In total, each contrast level was presented 36 times.

Insert Figure 2.

2.3.3. MRI acquisition

Experiments were performed using a whole-body 3-Tesla Philips Achieva MRI scanner at the Grenoble MRI facility IRMaGe in France. A 32 channel SENSE head coil was used for image acquisition. For functional scans, a gradient echo planar imaging (EPI MS-FFE) sequence was used with the following main parameters: TR/TE=2000/30ms, flip angle=80°, acquisition matrix=128x144, FOV=192x216, 25 transverse slices, slice thickness 1.5mm, with an acquisition/reconstruction voxel size=1.5x1.5x1.5mm. Slices were oriented to cover the structures implicated in the first steps of visual processing: the SC, LGN and the primary visual area (V1). One EPI image with the same parameters and covering all the brain (89 transverse slices) was acquired to eventually facilitate the realignment of functional and structural data. We acquired high-resolution structural images using a T1-weighted 3D MP-RAGE sequence with a spatial resolution of 1x1x1mm^3, 180 sagittal slices, acquisition matrix=256x240, TR/TE/TI=4.8/2.3/616ms and flip angle=9°. Finally, we used a T1-weighted FGATIR sequence with a spatial resolution of 0.75x0.75x1mm^3, transversal slices, acquisition matrix=268x233, TR/TE/TI=7.7/3.8/342ms and flip angle=8°, to facilitate the manual delineation of the LGN.

For brain perfusion measurement, the subjects were in a resting-state condition. A whole-brain pseudo-continous ASL (pCASL) sequence was performed with the following parameters: 1800 ms label, 1634 ms post-label delay and multi-slice single-shot EPI readout (3.5x3.5x5mm^3, 20 slices, TE/TR = 4230/12 ms). Thirty pCASL images plus an ASL reference scan and a T1 map were acquired for cerebral blood flow quantification.

For each subject the sequencing of the experiment was the following: five functional runs, 96 images each, one structural (MPRAGE) image, one whole brain EPI image, four functional runs, one structural (FGATIR) image and ASL perfusion imaging. During the acquisition, the subject was comfortably placed in a supine position with the head surrounded by soft foam to reduce head movements.

2.3.4. Physiological data acquisition

During each functional run acquisition, the cardiac signal was indirectly recorded at 100 Hz using a finger photoplethysmography (pulse plethysmography unit of the MR scanner), sensitive to the hemodynamic pulse at fingertip. The scanner software automatically recorded the maximum of

the plethysmographic signal (R-peak) and registered their occurrences and the marker of beginning and end of the fMRI acquisitions in the so-called ScanPhysLog file.

2.4. Psychophysical data analysis

The observer's choices associated with each trial from the psychophysical experiment were analyzed with the MLDS package (Knoblauch & Maloney, 2008, 2012) in the OpenSource software R (R Core Team, 2015) to obtain a perceptual response scale. The method uses a maximum likelihood criterion to estimate scale values that best predict observer's choices and generates a scale that has interval properties, i.e., equal differences in response are perceptually equal. The individual sessions of each group were averaged to obtain means and standard errors per group for the perceptual scale. Specific details on the procedure can be found elsewhere (Knoblauch & Maloney, 2012; Devinck, Gerardin, Dojat et al., 2014b).

2.5. Physiological data analysis

Heart rate variability (HRV) is an indicator of the cardiovascular activity. The spectral analysis of HRV provides a reliable and quantitative assessment of its fluctuations. Such an analysis was performed using a home-made program developed in R and detailed in (Rubio, Van Oudenhove, Pellissier et al., 2015). Briefly, the times corresponding to photoplethysmographic R-peaks were read from the ScanPhysLog file and the peak-to-peak intervals were computed. Aberrant values (outliers) could occur when the optical sensor localized at fingertip moved during the acquisition. Such outliers were automatically detected (values higher than the mean peak-to-peak value ±3 standard deviations) and replaced by the previous valid value. Peak-to-peak time series were resampled at the sampling frequency of the functional MRI i.e. 0.5 Hz and filtered using wavelet-transform in three low frequency (LF) sub-bands: the LF_{high}-HRV band from 0.12 to 0.25 Hz; the LF_{mid}-HRV band from 0.06 Hz to 0.12 Hz and the LF_{low}-HRV band from 0.03 to 0.06 Hz. The border effects and the time-shift introduced by the wavelet filtering were further corrected for. The three so-defined heart rate signals were further introduced in our model as covariates of non-interest.

2.6. MRI Data analysis: Individual analysis

Functional data analysis was performed using the single-participant general linear model (GLM) (Friston, Holmes, Worsley et al., 1995) for block-designs with SPM12 (Wellcome Department of Imaging Neuroscience, London, U.K.; http://www.fil.ion.ucl.ac.uk/spm) implemented in MATLAB. For each individual, functional volumes were first realigned to correct for head movements with a rigid body transformation using the first functional image acquired after the first structural scan as the reference. A mean functional volume was computed on which the whole brain EPI was realigned. The structural volumes (3D MP-RAGE and FGATIR) were then realigned to this volume. Times-series for each voxel were high-pass filtered (1/128 Hz cutoff) to remove low-frequency noise and signal drift. The random field theory we used for multiple comparison correction requires that the size of the spatial filter to smooth the data should be the same size as the spatial extend of the effect to be measured. We searched for clusters of activation in subcortical structures (SC and LGN) of small size, and then each functional volume was spatially slightly smoothed using a 2-mm FWHM (Full Width at Half Maximum) Gaussian kernel.

For each participant five conditions of interest (1%, 3%, 5%, 9% and fixation) were modeled as five regressors, constructed as boxcar functions convolved with a canonical hemodynamic response function. Movement parameters derived from realignment corrections (three translations and three rotations) were entered into the design matrix as additional nuisance factors. Including these factors led to an increase of the number of activated voxels. To specifically study the involvement of the first steps of visual information processing, we conducted a region-of-interest (ROI) analysis in SC, LGN and V1, individually defined. Left and right ROIs were functionally defined as contiguous clusters of activated voxels, i.e. voxels activated during all visual stimulation versus fixation condition ($p<0.001$ uncorrected). V1 was defined as the part of the occipital activation that lay in and around the calcarine sulcus. We considered that such a ROI delineation contain mainly voxels from V1 (and in part from V2). Additionally, for LGN and SC anatomical masks were manually delineated using MRICro software (Rorden & Brett, 2000), using respectively FGATIR and MPRAGE structural sequences and used to refine the LGN and SC ROI definition. Figure 3 shows examples of individual ROIs. In realigning each individual structural image to a reference space (MNI) with a non-linear high degree of freedom

transformation (Ashburner & Friston, 2005) we verified that our individual coordinates for SC and LGN were in accordance with those reported in the literature (O'Connor, Fukui, Pinsk et al., 2002; Schneider, Richter and Kastner, 2004; Schneider & Kastner, 2005; Schneider & Kastner, 2009) (see Supplementary Material: Table 1).

Insert Figure 3.

Contrast images were computed based on the GLM relative to each stimulus condition compared to the baseline (fixation) across all experimental runs. For each ROI (SC, LGN and V1) the voxels were sorted according to their response (t-statistic maps). Voxel number for each ROI was equated across individuals by restricting the pattern size to those voxels that showed a significant t-value ($p<0.001$ uncorrected). The number of voxels included for each individual ROI was 20 for SC, 80 for LGN and 200 for V1. For each subject voxels of contrast images were averaged in each ROI.

Similarly to functional data all individual ASL perfusion images were firstly realigned with a rigid transformation. A mean ASL image was then computed onto which the structural images, MPRAGE and FGATIR, were realigned. ASL signal amplitude was scaled in order to express the difference between control and tag images in units of ml/100g/min. Statistical maps were thresholded at $p<.05$ FWE-corrected for multiple comparisons. Finally, cerebral blood flow (CBF) measures were extracted from our primary ROIs (SC, LGN and V1) as well as from secondary ROIs (cingular, frontal, occipital, parietal and temporal cortex, insula and grey and white matters). These latter were extracted using a homemade atlas realigned to the structural image.

All further statistical analyses were performed using the statistical software Statistica for PC version 12 and the open source software R (R Core Team, 2015).

3. Results

3.1. Psychophysical data

3.1.1. *Estimated perceptual response to luminance contrast change*

A linear mixed-effect model with Contrast, c, as fixed effect and Subjects as random effect revealed a main effect of the contrast factor on the perceptual response estimated using the MLDS procedure ($p<10^{-15}$). To model this response, we consider the Michaelis-Menten function,

$$R = R_m \frac{c}{(c+\sigma)}$$

where R_m is the maximal response amplitude and σ is the contrast at which the response amplitude is half R_m (= semisaturation contrast). This model provides a reasonable description of the increase perceptual scale with the contrast luminance (see Figure 4a). The initial slope of the contrast response function is often estimated as $\frac{R_m}{\sigma}$ in electrophysiological studies, which is termed "contrast gain". This model correctly fits the contrast response function of cortical cells adapted from the Naka-Rushton equation (Naka & Rushton, 1968; Baylor, Hodgkin and Lamb, 1974). It was valid for each individual (see Supplementary Material: Figure 1).

3.1.2. *Age effect on the estimated perceptual response to contrast change*

A non-linear mixed-effect model with Age and Contrast as fixed effects and Subject as random effect revealed an interaction between Age and Contrast ($p<10^{-7}$) (see Figures 4b and 4c). Difference of contrast response varied significantly between groups. Nested likelihood ratio tests were used to compare the Michaelis-Menten model parameters between groups. Analyses showed that Rm and σ values for the oldest groups, i.e. Middle age and Elderly, differ significantly from the Young group values. Rm as well as σ parameters decreased with age (middle age and elderly vs young: $\Delta Rm = -3.24 \pm 1.19$, $p<.005$; $\Delta\sigma = -0.02 \pm 0.01$, $p<.05$) (for the values per group see Supplementary Material: Table 2).

Insert Figure 4.

3.2. Cerebral perfusion data

3.2.1. *Age effect on cerebral blood flow in primary ROIs*

Mean cerebral blood flow (CBF) across subjects for each group and ROIs (SC, LGN and V1) are reported in Table 1. A 3x3 analysis of variance (ANOVA) with Age as between-subjects factor and ROI as within-subjects factor revealed a main effect of ROI ($p<.10^{-3}$) but no main effect of age (p=.13). Post hoc analysis (Tuckey's HSD test) showed that participants present higher CBF values in V1 (56.46±18.30) compared to SC (48.82±19.77) (p<.01) and LGN (42.93±17.51) ($p<10^{-3}$) values (see Figure 5). The interaction Age x ROI did not reach significance (p=.11). No gender difference was observed (p=.16).

Insert Table1.

Note that a main effect of age was significant in other regions of the brain (Young CBF > Middle Age or Elderly CBF, p<.05): bilaterally for the cingular, frontal and parietal cortex, the right temporal cortex and globally for grey matter (see Supplementary Material: Figure 2).

Insert Figure 5.

3.3. fMRI data

3.3.1. Attentional task

Statistical analysis was performed on the average number of errors (= no detection or misdetection of the fixation cross orientation changes) at the attentional task. No difference between groups was observed (error rates: young = 5±1.1%; middle age = 6.35±0.8%; elderly = 3.9±0.9%, p=.76).

3.3.2. Bold responses to luminance contrast change

A main effect of contrast was observed for each ROI ($p<.10^{-5}$, Friedman analysis with contrast as within-subjects factor for each ROI), as illustrated in Figure 6. However, no effect of ROI was observed for each contrast (p>.5, Friedman analysis with ROI as within-subjects factor for each contrast). We performed *post hoc* comparisons using Wilcoxon rank test in each ROI to examine whether the luminance contrast level influenced the BOLD response. These analyses showed that, for each ROI, responses were significantly modulated by luminance contrast on the tested range ($1<3<5<9$, $p<10^{-5}$). No gender difference was observed (p>.1). Similar analyses performed in Hippocampus, a non-visual subcortical area, showed no effect of contrast on BOLD responses (p=.9), i.e. no modulation of its activity by the luminance contrast of the stimuli.

Insert Figure 6.

3.3.3. Age effect on the BOLD responses to luminance contrast change

Kruskall-Wallis analysis with age as between-subjects factor, conducted for each contrast in each ROI revealed a main effect of age in V1 for contrasts 3 to 9% and in LGN for contrasts 5 to 9% ($p<.005$), as illustrated in Figure 7. Indeed, a decrease of the response was observed for the Middle Age and Elderly participants compared to the Young participants for these two regions. A decrease of response with age was also observed in the SC but analysis of this effect only show a tendency for statistical significance ($p=0.07$). Post hoc comparisons were conducted using the Mann-Whitney U test in V1 and LGN. In LGN, results highlighted significant differences between Young and Middle Age ($p<.05$) and Young and Elderly ($p<.005$) participants for 5% and 9% contrast. Similarly, in V1, the analysis showed significant differences between Young and Middle Age ($p<.05$) and Young and Elderly ($p<.005$) participants for all luminance contrasts but 1%. The differences between Middle Age and Elderly participants for these contrasts were significant neither in LGN ($p>.1$) nor in V1 ($p>.2$).

Insert Figure 7.

Negative correlations between Age and BOLD response were detected using the Spearman correlation coefficient in V1 for 3% ($r = -0.65$, $p<10^{-3}$), 5% ($r = -0.73$, $p<10^{-4}$) and 9% ($r=-0.68$, $p<10^{-3}$) and in the LGN for 5% ($r = -0.69$, $p<10^{-3}$) and 9% ($r = -0.68$, $p<10^{-3}$) (see Figure 8).

Insert Figure 8.

3.3.4. Relation between BOLD responses and estimated perceptual responses to luminance contrast change

Positive correlations between BOLD responses and MLDS estimated perceptual responses to luminance contrast change were detected using the Spearman correlation coefficient for Young participants in LGN ($r = 0.41$, $p<.01$) and V1 ($r = 0.71$, $p<10^{-5}$); for Middle age participants in SC ($r = 0.42$, $p<.01$), LGN ($r = 0.39$, $p<.05$) and V1 ($r = 0.51$, $p<.01$) and for Elderly in SC ($r = 0.56$, $p<10^{-3}$), LGN ($r = 0.53$, $p<.01$) and V1 ($r = 0.57$, $p<.10^{-3}$). For young participants the BOLD

variance in SC was high (see Fig. 4) and the correlation with MLDS values was not significant. This may reflect a lack of statistical power.

4. Discussion

We clearly observed that BOLD responses increased with luminance contrast in our subcortical regions, the superior colliculus (SC) and the lateral geniculate nucleus (LGN), and in the primary visual cortex area V1. A statistically significant diminution was detected in LGN and V1 for older compared to younger participants, while basal perfusion remained unchanged. Additionally, perceptual responses, as assessed using the MLDS procedure, were correlated to fMRI measures in the three studied regions. Consequently, we assume that the BOLD signal modulation to luminance contrast variations we observed reflected brain activity modulation in normal ageing. Our fMRI-based methodology opens the way to the exploration of pathological differences in visual information processing at the subcortical level notably in neurodegenerative diseases.

4.1. An advanced framework for the non-invasive functional exploration of the Superior Colliculus

It is challenging to measure the functional activity of SC because of its small size, deep location and proximity to pulsating vascular structures, such as large blood vessels within and around the brainstem, potentially contaminating the BOLD signal. In this study, we solved these difficulties by introducing several methodological improvements. To allow accurate localization of activation in SC and limit partial volume effect, we used a 32-channel SENSE coil, a spatial resolution of 1.5 mm in each direction at 3T, with an acquisition volume centered on the SC structure.

Cardio-respiratory artifact removal. Several approaches to tackle possible vascular artifact may be introduced. In the first fMRI study of SC in human, Dubois and Cohen (DuBois & Cohen, 2000) used cardiac triggering of image acquisition to eliminate pulsatile motion effects *per se*. Each MRI image was acquired at the same point of the cardiac cycle lowering the effect of the cardiac noise. They introduced a T1 correction algorithm to compensate for the intensity variations produced by a variable TR. The remaining variation (1.5% of mean) was not harmful to observe retinotopic activation in SC but might be deleterious in case of weaker induced fMRI

responses. Correction for respiratory and cardio-respiratory artifacts was not considered. A second approach consists in the measure or estimation of the noise sources to define corresponding nuisance regressors. Wall et al. (Wall et al., 2009) proposed to estimate the noise from the mean time-course of voxels in a selected ROI during a rest scan. They assumed that fluctuations observed in the signal at rest reflected noise (physiological or technical) and entered the mean time-course in their statistical model as a nuisance regressor. The reference ROI was selected in the anterior cerebellum close to but not connected to SC. The interest of the approach is that no assumption about the source of noise is required. The drawback is that the reference ROI should be carefully chosen to be certain that the mean time-course does not contain a significant amount of signal related to the stimulus or reflecting functional connectivity. This is particularly relevant for visual stimulation for which a large network is activated.

In this study we assumed that the main source of noise hampering SC investigation was cardio-respiratory effects. We measured the cardiac signal (highly correlated >0.99 to respiratory rate, as measured using a pressure sensor positioned around the chest) and chose to introduce heart rate variability components as regressors of non-interest in our general linear model. Once the fMRI signal linked to the cardiovascular activity was removed, the only remaining signal reflected brain activity. The use of such regressors of nuisance is close to the approaches proposed in Limbrick et al. (Limbrick-Oldfield, Brooks, Wise et al., 2012) of a Physiological Noise Model derived from physiological recordings (cardiac and respiratory) and in Sylvester et al. (Sylvester et al., 2007) with the RETROICOR method based on pulse oximetry measurement. The coherence of the results we obtained indicates that the use of three regressors of nuisance extracted from a pulse oxymeter measurement may be sufficient to remove cardio-respiratory artifacts. The introduction of more regressors (33 in Limbrick et al. (Limbrick-Oldfield et al., 2012), 12 in Sylvester et al. (Sylvester et al., 2007)) might refine the results. Indeed, the number of significant voxels in SC reported by Limbrick-Oldfield et al. (Limbrick-Oldfield et al., 2012) seems higher than the number we detected (see their Fig 4). However, their method requires the setup of an ECG equipment for each subject and decreases the number of degree of freedom of the data model. Moreover, the increase of significant voxels they reported might be due to the stimulus they used (the luminance contrast was not specified) that provoked a large activation compared to our setting but did not allow the modulation of the activity (see below).

In the study of Wall et al. (Wall et al., 2009), the authors reported, for the population they considered (six young females), that the standard model for the hemodynamic response function as implemented in SPM (Friston et al., 1995) was suboptimal for SC but correct for V1 and LGN. Our data analysis using flexible models of hemodynamic response function (HRF) (finite impulse response approach) for the three groups of subjects did not confirm the need for a specific model of HRF for SC different from the one used for V1 and LGN. In the study of Gitelman et al. (Gitelman, Parrish, Friston et al., 2002) a canonical HRF was successfully used to search for SC activation correlations with visual search. To accurately investigate the form of the HRF in these three regions, methods for detection of brain activity combined with estimation of the hemodynamic response should be introduced (Chaari, Vincent, Forbes et al., 2013; Vincent, Badillo, Risser et al., 2014).

Age-effect on BOLD signal. In functional MR imaging, BOLD signal is considered as a direct and non-invasive index of brain activation. This signal reflects changes in hemodynamics parameters i.e. cerebral blood flow (CBF), cerebral blood volume and oxygen consumption following neural activation (Logothetis & Wandell, 2004). A number of factors, such as baseline blood flow, vascularization, vascular reactivity and neurovascular coupling, influence this signal and can evolve with age leading to alterations in the BOLD signal (see D'Esposito et al. (D'Esposito, Deouell and Gazzaley, 2003) for a review). Age-related vascular changes might then bias the straightforward attribution to a neural basis of age-related differences (Gauthier, Madjar, Desjardins-Crepeau et al., 2013).

We introduced a measurement of basal perfusion by ASL to make sure that the observed differences in the BOLD signal variations with age were due to the neuronal activity changes and not the consequence of a modification in the basal perfusion. We showed that CBF in resting state condition did not vary with age (see Figure 5) in our regions of interest. Note however that an age effect was observed in several other cortical regions: the bilateral cingular, frontal and parietal cortex, the right temporal cortex and the global grey matter (see Supplementary Material: Figure 2). CBF values obtained for V1 (see Table 1) are coherent with the literature (Chen, Rosas and Salat, 2011). To our knowledge, no values have been reported yet for SC and LGN. We observed higher CBF values in V1 compared to SC and LGN for each group (see Figure 5). This finding is consistent with the fact that cortical structures have a higher $\frac{Grey\ Matter\ (GM)}{White\ Matter\ (WM)}$ than subcortical structures and consequently a greater proportion of arteries, underlying higher CBF.

Moreover, a higher CBF value was measured in SC versus LGN (see Figure 5), which could be explained by the localization of SC close to prominent blood vessels such as the circle of Willis and the middle cerebral arteries. In recording perfusion imaging (ASL) at resting state, we missed the possible alteration with age of processes that couple demand during brain activation and vascular reactivity. To properly quantify cerebral perfusion differences, functional MR imaging of the vasoreactivity might be introduced (Krainik, Villien, Tropres et al., 2013) at the expense of the exam duration, a critical point in case of clinical study.

Some fMRI studies found that older adults have overall lower BOLD cortical responses depending on the task performed (D'Esposito et al., 2003; Ances, Liang, Leontiev et al., 2009; Kannurpatti, Motes, Rypma et al., 2010). This could be a confonding factor for V1 activation variations. However, it is unlikely that this factor was a covarying variable here. First, we found no basal perfusion difference between groups of varying age. Second, vascular contributions if any, as assessed by heart rate variability were introduced as nuisance cofactors in our statistical model. Third, the stimuli we used provoked strong retinotopic activity on early visual areas. In these areas no significant BOLD signal difference due to age was detected for such retinotopic stimulation (Chang, Yotsumoto, Salat et al., 2015).

Individual ROI analysis. Similarly to some studies (DuBois & Cohen, 2000; Schneider & Kastner, 2005; Sylvester et al., 2007; Wall et al., 2009), we opted for an individual ROI analysis of the functional data. We delineated for each participant three ROIs in SC, LGN and V1 based on functional and anatomical criteria (see Figure 3). Clearly, for the latter, the manual delineation introduced a subjective bias, not on the localization (see supplementary data Table 1), but on the size of the ROIs. Indeed, the mean volumes of SC and LGN ROIs in our study were incontestably smaller than those obtained using a delineation based on the retinotopy property of SC (Schneider & Kastner, 2005; Limbrick-Oldfield et al., 2012) and LGN (Schneider et al., 2004) or using flickering checkerboards with luminance constrast >10% (Schneider & Kastner, 2005). In these experiments, both magnocellular (M) and parvocellular (P) pathways were stimulated. Because P cells are known to outnumber M cells, notably in the LGN (Dreher, Fukada and Rodieck, 1976), this may explain the lower size of our LGN volumes. Note however that functional retinotopic mapping, allowing a proper delineation of these ROIS, requires a specific long lasting experiment (Bordier, Hupe and Dojat, 2015), unadapted to clinical studies, our next objective.

4.2. Aging effect on subcortical and cortical processing of the low luminance contrast

With such a framework, we successfully recorded a progressive increase of BOLD responses as a function of luminance contrast (<10%) in SC, LGN and V1 (see Figure 6), with a stronger modulation for V1, as previously reported by (Boynton, Demb, Glover et al., 1999). For SC, our results are consistent with the literature (Kastner, O'Connor, Fukui et al., 2004; Schneider & Kastner, 2005; Schneider & Kastner, 2009) as we show a modulation of SC responses to low contrast. We also extended those results with the use of luminance contrasts below 5%. To demonstrate the validity of our fMRI protocol to reveal potential visual dysfunction, we then explored the effect of aging as the visual system is well known to change with age, at least at a cortical level. Middle age and elderly participants had a visual exam by an ophthalmologist before the experiments. All participants had a normal or corrected-to-normal vision, therefore eye alterations can be ruled out in the effect observed.

For V1 and LGN a statistically significant decrease of neural activation is observed (see Figure 7), which is linear with age for the luminance contrast range of 1-9% (see Figure 8). Such a decrease of neural activity in our ROIs is consistent with structural brain alterations with aging. For V1, a significant decrease of the surface area (Brewer & Barton, 2012a) and a reduced response to visual stimulation (Crossland, Morland, Feely et al., 2008) were reported when comparing aging and young subjects. Yuang et al. (Yang, Liang, Guangxing et al., 2009) showed that the optimal spatial frequency and spatial resolution were decreased in aged monkeys in both V1 and MT, which seems to indicate that the influence of aging on V1 is not compensated by higher-order visual cortices but rather extends along the visual processing pathway. Age-related structural changes were also observed in LGN with a progressive decrease in size from 20 to 65 years old in Human (Li, He, Shi et al., 2012), coherent with data from animal studies showing a LGN degeneration in normal aging (neuronal volume attenuation and neuron diameter reduction) (Diaz, Villena, Gonzalez et al., 1999), although the spatial and temporal properties of LGN neurons seem preserved in elderly monkeys (Spear, Moore, Kim et al., 1994). However, no study confirms this preservation in human.

For SC, the integrative centers (Sparks, 1988) could be affected by age, as demonstrated by the stereological study of Diaz (Diaz et al., 1999) in old rats, highlighting a process of somatic and nuclear atrophy in superficial layer neurons implicated in vision. Again, no human data are available. In SC a non-statistically significant decrease in BOLD response with age was

observed. This finding could be due first to the small number of voxels available for the measure, second to the insufficient number of retinal cells that project to SC (10%) to bring out any age effect, and the absence of repercution of the age-modulated information coming from the M-layers projections from LGN to SC (Hoffmann, 1973). An alternative hypothesis concerning the apparent preservation of the SC functional modulation by low contrasts with age is that our results reflect in fact the preserved unconscious visual part of the SC functional activity. Indeed, based on the "blindsight" syndrome, it has been shown that patients with bilateral occipital damage retained some visual capacities (Weiskrantz, 1986), supported by residual networks not disturbed by the cortical lesion, such as the retino-tectal pathway, that bypassed V1, a crucial area in visual awareness (Weiskrantz, Warrington, Sanders et al., 1974; Weiskrantz, 1986).

SC is a structure that plays a preponderent role in visual attention. It is conceivable that aging altered the SC conscious activity, but because of the load required by our attentional task, i.e. the fixation of the central cross, the modulation of the SC conscious activity by our visual stimulus was then masked. In contrary, our results might indicate that the SC unconscious activity might be preserved with age and modulated by checkerboards varying in luminance reflecting the functional integrity of the SC unconscious retino-tectal visual pathway with age. The use of transcranial magnetic stimulation, with transient blockade of the unconscious visual pathway without suppression of the conscious visual pathway (Ro, Shelton, Lee et al., 2004; Jolij & Lamme, 2005; Allen, Sumner and Chambers, 2014), may be an interesting neurophysiological approach to understand how conscious and unconscious visual pathways contribute to an age-related sensitivity loss in SC. It would also add important information on the influence of the visual cortex on SC activity.

4.3. Aging effect on luminance contrast perception

In Boynton et al. (Boynton et al., 1999) contrast response functions measured using fMRI were found to be consistent with psychophysical data (paired-comparison) in several visual areas (V1, V2d, V3d and V3A). Subcortical areas were not explored. Paired-comparison methods have been extended to estimate perceptual scales within a signal detection framework (Maloney & Yang, 2003; Ho, Landy and Maloney, 2009). A maximum likelihood criterion is then introduced to estimate interval scales that best predict observers' choices. Recently, Maloney and colleagues introduced the Maximum Likelihood Difference Scaling (MLDS) procedure task (Maloney &

Yang, 2003; Knoblauch & Maloney, 2008; Knoblauch & Maloney, 2012). This method appears to be robust indicating, as well, how the sensitivity of the observer varies to each stimulus magnitude. It has been successfully applied to characterize color differences (Lindsey, Brown, Reijnen et al., 2010), surface glossiness (Obein, Knoblauch and Vienot, 2004; Emrith, Chantler, Green et al., 2010), image quality (Charrier, Maloney, Cherifi et al., 2007), adaptative process of face distortion, neural encoding of sensory attributes (Yang, Szeverenyi and Ts'o, 2008) and more recently to measure the strength of the watercolor effect, where an irregular chromatic contour generates a color percept that looks like a uniform color surface, as a function of luminance elevation of the inner contour (Devinck & Knoblauch, 2012). Here, we used MLDS procedure task to estimate luminance contrast perception. Clearly, the recorded data showed a modulation of the perceptual response as a function of luminance contrast from 2% to 15%, approaching an asymptote near 20%. We have also shown that our fMRI evaluation was consistent with those psychophysical data. Indeed, we found significant positive correlations between BOLD responses and MLDS estimated perceptual responses to luminance contrast change in our ROIs.

In order to modulate SC response, we designed our stimuli to preferentially activate the M pathway using both low spatial frequency and luminance contrast (from 2% to 20%). This was clearly confirmed by the Michaelis-Menten function that perfectly fitted the estimated perceptual response to luminance contrast variations (see Figure 4). Indeed, this function was used to describe the contrast gain signatures of M cells in the retina (Lee, Pokorny, Smith et al., 1990) and LGN (Kaplan & Shapley, 1986). The M pathway is characterized by a logarithmic response curve, i.e. high contrast gain and saturation at relatively low levels of contrast, whereas the P pathway provides a linear response, i.e. low contrast gain and a linear response to luminance contrast variations (Kaplan & Shapley, 1986; Merigan & Maunsell, 1990). Many studies have reported contrast sensitivity decline with age. For Owsley et al. (Owsley et al., 1983), contrast sensitivity for stationary low spatial frequency stimuli remained the same throughout adulthood, whereas sensitivity for stationary high spatial frequency stimuli decreased with age, suggesting more pronounced impairment of the P pathway. Similarly, Elliot and Werner (Elliott & Werner, 2010) investigated separately M and P pathways based on their contrast gain signature (Pokorny & Smith, 1997) and reported a more pronounced functional deficit of the P pathway with age. More recently, Ramanoel et al. (Ramanoel, Kauffmann, Cousin et al., 2015) investigated the

effects of normal aging on spatial frequency processing during natural visual scenes categorization. They reported a low-contrast deficit in normal elderly population only for high spatial frequency again suggesting more age influence on the P pathway.

While most studies have highlighted functional changes in normal aging for the P pathway, which are confirmed in the present experiment, the literature is more controversial concerning possible M pathway deficits with aging (Owsley, 2011). Our data (Figure 4b) indicate an effect of age on luminance contrast perception for values from 2 to 15%. Consequently, they confirm for low spatial frequency stimuli (<1.6 cpd) that this age effect on luminance contrast perception is on the P pathway, preferentially activated by luminance contrasts above 10%, but also on the M pathway, more sensitive to luminance contrasts below 10% (Merigan & Eskin, 1986). This observation is coherent with the McKendrick study (McKendrick, Sampson, Walland et al., 2007), showing a reduction of contrast sensitivity for low spatial frequency of both the M and P pathways. Moreover, Bordaberry and al. (Bordaberry, Lenoble and Delord, 2012) highlighted a differential functional loss for M and P pathways. Indeed, the M deficit is lower at the beginning of aging but keep deteriorating after 75 years old while the P deficit is larger at the beginning of aging and more stable from 60 years old. It is important to note that a clean disambiguation of M and P responses is difficult to achieve (Skottun & Skoykes, 2011). Temporal frequency processing is preferentially supported by the M pathway (Kaplan & Shapley, 1986). Kim and Mayer (Kim & Mayer, 1994) observed a sensitivity decrease for low spatial frequency flickering stimuli in elderly when the temporal frequency increased. Based on the data presented in the study of Elliott and Werner (Elliott & Werner, 2010), the flickering frequency of 4Hz we used for our checkerboards might be sufficiently high to alter the response in V1 and LGN for middle age and elderly participants. However, the good correlation between neural correlates and perceptual scales, as estimated from observations of static checkerboards, allows us to rule out an influence of the temporal frequency component in the observed deficits with age in response to luminance contrast modulation.

4.4. Conclusion

Taken together, fMRI and psychophysics results indicate that both M and P pathways may play a role in age-related luminance contrast sensitivity loss. Understanding the mechanisms underlying these changes occurring in normal aging is essential both for understanding the normal aging

process and for comparisons between healthy aging subjects and aging patients with age-related visual and/or cortical/subcortical disorders. In particular improving our knowledge about the functioning of the superior colliculus may help to distinguish changes related to healthy aging from those resulting of neurodegenerative processes such as Parkinson's (Kim and Hikosaka, 2015) or Hungtinton's (Rupp et al., 2012) diseases but also in patients with Attention deficit hyperactivity disorder (ADHD) (Overton, 2008). The methodology we propose combining fMRI and psychophysics will allow performing such investigations.

Acknowledgments

Emmanuelle Bellot is recipient of a grant from the Université Grenoble Alpes. This work was partly supported by a grant from 'La Fondation de l'Avenir' (France). The Grenoble MRI facility IRMaGe was partly funded by the French program 'Investissement d'Avenir' run by the Agence Nationale pour la Recherche (ANR-11-INBS-0006). Kenneth Knoblauch was partly supported by a grant from the Agence Nationale de la Recherche, LABEX CORTEX (ANR-11-LABX-0042). The authors thank Chantal Delon-Martin for help with physiological data analysis and Irène Troprès for assistance in MR sequence development.

References

Allard, R., Renaud, J., Molinatti, S.and Faubert, J. (2013). Contrast sensitivity, healthy aging and noise. *Vision Res*, *92*, 47-52.

Allen, C. P., Sumner, P.and Chambers, C. D. (2014). The timing and neuroanatomy of conscious vision as revealed by TMS-induced blindsight. *J Cogn Neurosci*, *26*(7), 1507-1518.

Ances, B. M., Liang, C. L., Leontiev, O., Perthen, J. E., Fleisher, A. S., Lansing, A. E.and Buxton, R. B. (2009). Effects of aging on cerebral blood flow, oxygen metabolism, and blood oxygenation level dependent responses to visual stimulation. *Hum Brain Mapp*, *30*(4), 1120-1132.

Ashburner, J.and Friston, K. J. (2005). Unified segmentation. *Neuroimage*, *26*(3), 839-851.

Atchley, P.and Andersen, G. J. (1998). The effect of age, retinal eccentricity, and speed on the detection of optic flow components. *Psychol Aging*, *13*(2), 297-308.

Ball, K., Edwards, J. D.and Ross, L. A. (2007). The impact of speed of processing training on cognitive and everyday functions. *J Gerontol B Psychol Sci Soc Sci*, *62 Spec No 1*, 19-31.

Baylor, D. A., Hodgkin, A. L.and Lamb, T. D. (1974). The electrical response of turtle cones to flashes and steps of light. *J Physiol*, *242*(3), 685-727.

Benevento, L. A.and Fallon, J. H. (1975). The ascending projections of the superior colliculus in the rhesus monkey (Macaca mulatta). *J Comp Neurol*, *160*(3), 339-361.

Benevento, L. A.and Yoshida, K. (1981). The afferent and efferent organization of the lateral geniculo-prestriate pathways in the macaque monkey. *J Comp Neurol*, *203*(3), 455-474.

Bordaberry, P., Lenoble, Q.and Delord, S. (2012). [Aging of visual object recognition: interaction between a "spatial frequency-specific" deficit and a "category-specific" deficit]. *Geriatr Psychol Neuropsychiatr Vieil*, *10*(4), 453-462.

Bordier, C., Hupe, J. M.and Dojat, M. (2015). Quantitative evaluation of fMRI retinotopic maps, from V1 to V4, for cognitive experiments. *Front Hum Neurosci*, *9*, 277.

Boynton, G. M., Demb, J. B., Glover, G. H.and Heeger, D. J. (1999). Neuronal basis of contrast discrimination. *Vision Res*, *39*(2), 257-269.

Brace, L. R., Kraev, I., Rostron, C. L., Stewart, M. G., Overton, P. G.and Dommett, E. J. (2015). Altered visual processing in a rodent model of Attention-Deficit Hyperactivity Disorder. *Neuroscience*, *303*, 364-377.

Brainard, D. H. (1997). The Psychophysics Toolbox. *Spat Vis*, *10*(4), 433-436.

Brewer, A. A.and Barton, B. (2012a). Effects of healthy aging on human primary visual cortex. *Health*, *4*, 695-702.

Chaari, L., Vincent, T., Forbes, F., Dojat, M.and Ciuciu, P. (2013). Fast joint detection-estimation of evoked brain activity in event-related FMRI using a variational approach. *IEEE Trans Med Imaging*, *32*(5), 821-837.

Chang, L. H., Yotsumoto, Y., Salat, D. H., Andersen, G. J., Watanabe, T.and Sasaki, Y. (2015). Reduction in the retinotopic early visual cortex with normal aging and magnitude of perceptual learning. *Neurobiol Aging*, *36*(1), 315-322.

Charrier, C., Maloney, L. T., Cherifi, H.and Knoblauch, K. (2007). Maximum likelihood difference scaling of image quality in compression-degraded images. *J Opt Soc Am A Opt Image Sci Vis*, *24*(11), 3418-3426.

Chen, J. J., Rosas, H. D.and Salat, D. H. (2011). Age-associated reductions in cerebral blood flow are independent from regional atrophy. *NeuroImage* *55*, 468-478.

Crossland, M. D., Morland, A. B., Feely, M. P., von dem Hagen, E.and Rubin, G. S. (2008). The effect of age and fixation instability on retinotopic mapping of primary visual cortex. *Invest Ophthalmol Vis Sci*, *49*(8), 3734-3739.

Cynader, M.and Berman, N. (1972). Receptive-field organization of monkey superior colliculus. *J Neurophysiol*, *35*(2), 187-201.

D'Esposito, M., Deouell, L. Y.and Gazzaley, A. (2003). Alterations in the BOLD fMRI signal with ageing and disease: a challenge for neuroimaging. *Nat Rev Neurosci*, *4*(11), 863-872.

Denison, R. N., Vu, A. T., Yacoub, E., Feinberg, D. A.and Silver, M. A. (2014). Functional mapping of the magnocellular and parvocellular subdivisions of human LGN. *Neuroimage*, *102 Pt 2*, 358-369.

Derrington, A. M.and Lennie, P. (1984). Spatial and temporal contrast sensitivities of neurones in lateral geniculate nucleus of macaque. *J Physiol*, *357*, 219-240.

Devinck, F., Gerardin, P., Dojat, M.and Knoblauch, K. (2014b). Spatial selectivity of the watercolor effect. *Journal of the Optical Society of America A, Optics, image science and vision*, *31*, 1-6.

Devinck, F.and Knoblauch, K. (2012). A common signal detection model accounts for both perception and discrimination of the watercolor effect. *J Vis*, *12*(3).

Diaz, F., Villena, A., Gonzalez, P., Requena, V., Rius, F.and Perez De Vargas, I. (1999). Stereological age-related changes in neurons of the rat dorsal lateral geniculate nucleus. *Anat Rec*, *255*(4), 396-400.

Dreher, B., Fukada, Y.and Rodieck, R. W. (1976). Identification, classification and anatomical segregation of cells with X-like and Y-like properties in the lateral geniculate nucleus of old-world primates. *J Physiol*, *258*(2), 433-452.

DuBois, R. M.and Cohen, M. S. (2000). Spatiotopic organization in human superior colliculus observed with fMRI. *Neuroimage*, *12*(1), 63-70.

Elliott, D., Whitaker, D.and MacVeigh, D. (1990). Neural contribution to spatiotemporal contrast sensitivity decline in healthy ageing eyes. *Vision Res*, *30*(4), 541-547.

Elliott, D. B. (1987). Contrast sensitivity decline with ageing: a neural or optical phenomenon? *Ophthalmic Physiol Opt*, *7*(4), 415-419.

Elliott, S. L.and Werner, J. S. (2010). Age-related changes in contrast gain related to the M and P pathways. *J Vis*, *10*(4), 4 1-15.

Emrith, K., Chantler, M. J., Green, P. R., Maloney, L. T.and Clarke, A. D. (2010). Measuring perceived differences in surface texture due to changes in higher order statistics. *J Opt Soc Am A Opt Image Sci Vis*, *27*(5), 1232-1244.

Felleman, D. J.and Van Essen, D. C. (1991). Distributed hierarchical processing in the primate cerebral cortex. *Cereb Cortex*, *1*(1), 1-47.

Fries, W. (1984). Cortical projections to the superior colliculus in the macaque monkey: a retrograde study using horseradish peroxidase. *J Comp Neurol*, *230*(1), 55-76.

Friston, K. J., Holmes, A., Worsley, K., Poline, J.-B., Frith, C.and Frackowiak, R. (1995). Statistical parametric maps in functional imaging : a general linear approach. Human Brain Mapping. *Human Brain Mapping*, *2*, 189-210.

Gauthier, C. J., Madjar, C., Desjardins-Crepeau, L., Bellec, P., Bherer, L.and Hoge, R. D. (2013). Age dependence of hemodynamic response characteristics in human functional magnetic resonance imaging. *Neurobiol Aging*, *34*(5), 1469-1485.

Gitelman, D. R., Parrish, T. B., Friston, K. J.and Mesulam, M. M. (2002). Functional anatomy of visual search: regional segregations within the frontal eye fields and effective connectivity of the superior colliculus. *Neuroimage*, *15*(4), 970-982.

Hendrickson, A., Wilson, M. E.and Toyne, M. J. (1970). The distribution of optic nerve fibers in Macaca mulatta. *Brain Res*, *23*(3), 425-427.

Ho, Y.-X., Landy, M. S.and Maloney, L. T. (2009). Conjoint measurement of gloss and surface texture. *Psychol Sci.*, *19*(2), 196-204.

Hoffmann, K. P. (1973). Conduction velocity in pathways from retina to superior colliculus in the cat : a correlation with receptive-field properties. *J Neurophysiol*, *36*, 409-424.

Jolij, J.and Lamme, V. A. (2005). Repression of unconscious information by conscious processing: evidence from affective blindsight induced by transcranial magnetic stimulation. *Proc Natl Acad Sci U S A*, *102*(30), 10747-10751.

Kannurpatti, S. S., Motes, M. A., Rypma, B.and Biswal, B. B. (2010). Neural and vascular variability and the fMRI-BOLD response in normal aging. *Magn Reson Imaging*, *28*(4), 466-476.

Kaplan, E.and Shapley, R. M. (1986). The primate retina contains two types of ganglion cells, with high and low contrast sensitivity. *Proc Natl Acad Sci U S A*, *83*(8), 2755-2757.

Kastner, S., O'Connor, D. H., Fukui, M. M., Fehd, H. M., Herwig, U.and Pinsk, M. A. (2004). Functional imaging of the human lateral geniculate nucleus and pulvinar. *J Neurophysiol*, *91*(1), 438-448.

Kaytal, S., Zughni, S., Greene, C.and Ress, D. (2010). Topography of Covert Visual Attention in Human Superior Colliculus. *J Neurophysiol*, *104*, 3074-3083.

Kim, C. B. and Mayer, M. J. (1994). Foveal flicker sensitivity in healthy aging eyes. II. Cross-sectional aging trends from 18 through 77 years of age. *J Opt Soc Am A Opt Image Sci Vis*, *11*(7), 1958-1969.

Kim, H.F. and Hikosaka, O. (2015) Parallel basal ganglia circuits for voluntary and automatic behaviour to reach rewards. *Brain* 138, 1776-1800.

Knoblauch, K.and Maloney, L. T. (2008). MLDS : Maximum likelihood difference scaling in R. *Journal of Statistical Software*, *25*, 1-26.

Knoblauch, K.and Maloney, L. T. (2012). *Modeling psychophysical data in R*: New-York:Springer.

Knoblauch, K., Saunders, F., Kusuda, M., Hynes, R., Podgor, M., Higgins, K. E.and de Monasterio, F. M. (1987). Age and illuminance effects in the Farnsworth-Munsell 100-hue test. *Appl Opt*, *26*(8), 1441-1448.

Knoblauch, K., Vital-Durand, F.and Barbur, J. L. (2001). Variation of chromatic sensitivity across the life span. *Vision Res*, *41*(1), 23-36.

Krainik, A., Villien, M., Tropres, I., Attye, A., Lamalle, L., Bouvier, J., Pietras, J., Grand, S., Le Bas, J. F.and Warnking, J. (2013). Functional imaging of cerebral perfusion. *Diagn Interv Imaging*, *94*(12), 1259-1278.

Kunzle, H.and Akert, K. (1977). Efferent connections of cortical, area 8 (frontal eye field) in Macaca fascicularis. A reinvestigation using the autoradiographic technique. *J Comp Neurol*, *173*(1), 147-164.

Kuypers, H. G.and Lawrence, D. G. (1967). Cortical projections to the red nucleus and the brain stem in the Rhesus monkey. *Brain Res*, *4*(2), 151-188.

Lee, B. B., Pokorny, J., Smith, V. C., Martin, P. R.and Valberg, A. (1990). Luminance and chromatic modulation sensitivity of macaque ganglion cells and human observers. *J Opt Soc Am A*, *7*(12), 2223-2236.

Li, M., He, H. G., Shi, W., Li, J., Lv, B., Wang, C. H., Miao, Q. W., Wang, Z. C., Wang, N. L., Walter, M.and Sabel, B. A. (2012). Quantification of the human lateral geniculate nucleus in vivo using MR imaging based on morphometry: volume loss with age. *AJNR Am J Neuroradiol*, *33*(5), 915-921.

Limbrick-Oldfield, E. H., Brooks, J. C., Wise, R. J., Padormo, F., Hajnal, J. V., Beckmann, C. F.and Ungless, M. A. (2012). Identification and characterisation of midbrain nuclei using optimised functional magnetic resonance imaging. *Neuroimage*, *59*(2), 1230-1238.

Lindsey, D. T., Brown, A. M., Reijnen, E., Rich, A. N., Kuzmova, Y. I.and Wolfe, J. M. (2010). Color channels, not color appearance or color categories, guide visual search for desaturated color targets. *Psychol Sci*, *21*(9), 1208-1214.

Linzenbold, W., Lindig, T.and Himmelbach, M. (2011). Functional neuroimaging of the oculomotor brainstem network in humans. *Neuroimage*, *57*(3), 1116-1123.

Logothetis, N. K.and Wandell, B. A. (2004). Interpreting the BOLD signal. *Annu Rev Physiol*, *66*, 735-769.

Lux, S., Marshall, J. C., Thimm, M.and Fink, G. R. (2008). Differential processing of hierarchical visual stimuli in young and older healthy adults: implications for pathology. *Cortex*, *44*(1), 21-28.

Maloney, L. T.and Yang, J. N. (2003). Maximum Likelihood Difference Scaling. *Journal of Vision*, *3*(8), 573-585.

Marrocco, R. T.and Li, R. H. (1977). Monkey superior colliculus: properties of single cells and their afferent inputs. *J Neurophysiol*, *40*(4), 844-860.

McKendrick, A. M., Sampson, G. P., Walland, M. J.and Badcock, D. R. (2007). Contrast sensitivity changes due to glaucoma and normal aging: low-spatial-frequency losses in both magnocellular and parvocellular pathways. *Invest Ophthalmol Vis Sci*, *48*(5), 2115-2122.

Merigan, W. H.and Eskin, T. A. (1986). Spatio-temporal vision of macaques with severe loss of P beta retinal ganglion cells. *Vision Res*, *26*(11), 1751-1761.

Merigan, W. H.and Maunsell, J. H. (1990). Macaque vision after magnocellular lateral geniculate lesions. *Vis Neurosci*, *5*(4), 347-352.

Merigan, W. H.and Maunsell, J. H. R. (1990). Macaque vision after magnocellular lateral geniculate lesions. *Visual Neuroscience*, *5*, 347-352.

Naka, K. I.and Rushton, W. A. (1968). S-potential and dark adaptation in fish. *J Physiol*, *194*(1), 259-269.

O'Connor, D. H., Fukui, M. M., Pinsk, M. A.and Kastner, S. (2002). Attention modulates responses in the human lateral geniculate nucleus. *Nat Neurosci*, *5*(11), 1203-1209.

Obein, G., Knoblauch, K.and Vienot, F. (2004). Difference scaling of gloss: nonlinearity, binocularity, and constancy. *J Vis*, *4*(9), 711-720.

Overton, P. G. (2008). Collicular dysfunction in attention deficit hyperactivity disorder. *Med Hypotheses*, *70*(6), 1121-1127.

Owsley, C. (2011). Aging and vision. *Vision Res*, *51*(13), 1610-1622.

Owsley, C., Sekuler, R.and Siemsen, D. (1983). Contrast sensitivity throughout adulthood. *Vision Res*, *23*(7), 689-699.

Peirce, J. W. (2007). PsychoPy--Psychophysics software in Python. *J Neurosci Methods*, *162*(1-2), 8-13.

Peirce, J. W. (2009). Generating stimuli for neuroscience using PsychoPy. *Front Neuroinform*, *15*(2).

Pelli, D. G. (1997). The VideoToolbox software for visual psychophysics: transforming numbers into movies. *Spat Vis*, *10*(4), 437-442.

Pokorny, J.and Smith, V. C. (1997). Psychophysical signatures associated with magnocellular and parvocellular pathway contrast gain. *J Opt Soc Am A Opt Image Sci Vis*, *14*(9), 2477-2486.

Poncelet, B. P., Wedeen, V. J., Weisskoff, R. M.and Cohen, M. S. (1992). Brain parenchyma motion: measurement with cine echo-planar MR imaging. *Radiology*, *185*(3), 645-651.

R Core Team (2015). *R : A language and environment for statistical computing*. Vienna, Austria: R Foundation for Statistical Computing.

Ramanoel, S., Kauffmann, L., Cousin, E., Dojat, M.and Peyrin, C. (2015). Age-Related Differences in Spatial Frequency Processing during Scene Categorization. *PLoS One*, *10*(8), e0134554.

Ro, T., Shelton, D., Lee, O. L.and Chang, E. (2004). Extrageniculate mediation of unconscious vision in transcranial magnetic stimulation-induced blindsight. *Proc Natl Acad Sci U S A*, *101*(26), 9933-9935.

Rolland, M., Carcenac, C., Overton, P. G., Savasta, M.and Coizet, V. (2013). Enhanced visual responses in the superior colliculus and subthalamic nucleus in an animal model of Parkinson's disease. *Neuroscience*, *252*, 277-288.

Rorden, C.and Brett, M. (2000). Stereotaxic display of brain lesions. *Behav Neurol*, *12*(4), 191-200.

Rubio, A., Van Oudenhove, L., Pellissier, S., Ly, H. G., Dupont, P., Lafaye de Micheaux, H., Tack, J., Dantzer, C., Delon-Martin, C.and Bonaz, B. (2015). Uncertainty in

anticipation of uncomfortable rectal distension in modulated by the autonomic nervous system - A fMRI study in healthy volunteers. *NeuroImage* *107*, 10-22.

Rupp, J., Dzemidzic, M., Blekher, T., West, J., Hui, S., Wojcieszek, J., Saykin, A. J., Kareken, D. A.and Foroud, T. (2012). Comparison of vertical and horizontal saccade measures and their relation to gray matter changes in premanifest and manifest Huntington disease. *J Neurol*, *259*(2), 267-276.

Schiller, P. H.and Koerner, F. (1971). Discharge characteristics of single units in superior colliculus of the alert rhesus monkey. *J Neurophysiol*, *34*(5), 920-936.

Schiller, P. H.and Malpeli, J. G. (1977). Properties and tectal projections of monkey retinal ganglion cells. *J Neurophysiol*, *40*(2), 428-445.

Schneider, K. A.and Kastner, S. (2005). Visual responses of the human superior colliculus: a high-resolution functional magnetic resonance imaging study. *J Neurophysiol*, *94*(4), 2491-2503.

Schneider, K. A.and Kastner, S. (2009). Effects of sustained spatial attention in the human lateral geniculate nucleus and superior colliculus. *J Neurosci*, *29*(6), 1784-1795.

Schneider, K. A., Richter, M. C.and Kastner, S. (2004). Retinotopic organization and functional subdivisions of the human lateral geniculate nucleus: a high-resolution functional magnetic resonance imaging study. *J Neurosci*, *24*(41), 8975-8985.

Sherman, S. M.and Guillery, R. W. (2006). *Exploring the Thalamus and Its Role in Cortical Function*. Cambridge, MA: MIT Press.

Sherman, S. M.and Koch, C. (1986). The control of retinogeniculate transmission in the mammalian lateral geniculate nucleus. *Exp Brain Res*, *63*(1), 1-20.

Skottun, B. C.and Skoykes, J. R. (2011). On identifying magnocellular and parvocellular responses on the basis of contrast-response functions. *Schizophrenia Bulletin*, *37*(1), 23-26.

Sparks, D. L. (1988). Saccadic command signals in the superior colliculus: implications for sensorimotor transformations. *Can J Physiol Pharmacol*, *66*(4), 527-531.

Spear, P. D., Moore, R. J., Kim, C. B., Xue, J. T.and Tumosa, N. (1994). Effects of aging on the primate visual system: spatial and temporal processing by lateral geniculate neurons in young adult and old rhesus monkeys. *J Neurophysiol*, *72*(1), 402-420.

Sylvester, R., Jiosephs, O., Driver, J.and Rees, G. (2007). Visual fMRI Responses in Human Superior Colliculus Show a Temporal-Nasal Asymmetry That Is Absent in Lateral Geniculate and Visual Cortex. *J Neurophysiol*, *97*, 1495-1502.

Vincent, T., Badillo, S., Risser, L., Chaari, L., Bakhous, C., Forbes, F.and Ciuciu, P. (2014). Flexible multivariate hemodynamics fMRI data analyses and simulations with PyHRF. *Front Neurosci*, *8*, 67.

Wall, M. B., Walker, R.and Smith, A. T. (2009). Functional imaging of the human superior colliculus: an optimised approach. *Neuroimage*, *47*(4), 1620-1627.

Wang, Y., Zhou, Y., Ma, Y.and Leventhal, A. G. (2005). Degradation of signal timing in cortical areas V1 and V2 of senescent monkeys. *Cereb Cortex*, *15*(4), 403-408.

Weiskrantz, L. (1986). *A case study and implications.* Oxford: Oxford University press.

Weiskrantz, L., Warrington, E., Sanders, M.and Marshall, J. (1974). Visual capacity in hemianopic field following a restricted occipital ablation. *Brain*, *97*, 709-728.

Wilson, M. E.and Toyne, M. J. (1970). Retino-tectal and cortico-tectal projections in Macaca mulatta. *Brain Res*, *24*(3), 395-406.

Yang, J. N., Szeverenyi, N. M.and Ts'o, D. (2008). Neural resources associated with perceptual judgment across sensory modalities. *Cereb Cortex*, *18*(1), 38-45.

Yang, Y., Liang, Z., Guangxing, L., Yongchang, W.and Yifeng, Z. (2009). Aging affects response variability of V1 and MT neurons in rhesus monkeys. *Brain Research*, *1274*, 21-27.

Yang, Y., Liang, Z., Li, G., Wang, Y., Zhou, Y.and Leventhal, A. G. (2008). Aging affects contrast response functions and adaptation of middle temporal visual area neurons in rhesus monkeys. *Neuroscience*, *156*(3), 748-757.

Yang, Y., Zhang, J., Liang, Z., Li, G., Wang, Y., Ma, Y., Zhou, Y.and Leventhal, A. G. (2009). Aging affects the neural representation of speed in Macaque area MT. *Cereb Cortex*, *19*(9), 1957-1967.

Yu, S., Wang, X., Fu, Y., Zhang, L., Ma, Y., Wang, Y.and Zhou, Y. (2005). Effects of age on latency and variability of visual response in monkeys. *Chinese Science Bulletin*, *50*(11), 1163-1165.

Zhang, P., Zhou, H., Wen, W.and He, S. (2015). Layer-specific response properties of the human lateral geniculate nucleus and superior colliculus. *Neuroimage*, *111*, 159-166.

Figures captions

Figure 1. MLDS experiment: Example of a triad used in the psychophysical session before scanning. The observer had to fixate each pattern until he/she could choose which of the two bottom patterns (left or right) was most similar to the upper pattern with respect to the color of its interior region.

Figure 2. fMRI protocol and visual stimuli. Top: visual stimuli, achromatic checkerboards hemifield (0.42 cpd) varying in luminance (1-9%) and flashing at a frequency of 4 Hz. Below: experimental paradigm, a block-design paradigm with the four luminance contrast levels (1, 3, 5 and 9%) interleaved with fixation intervals.

Figure 3. The regions of interest for one participant. Functional mask: individual functional activation obtained for all visual stimuli relative to fixation is projected onto the corresponding structural T1-weighted image. Anatomical mask is manually delineated in 3D (cyan line) and used to refine the ROIs definition. From left to right: Superior Colliculus, Lateral Geniculate Nucleus, and V1 regions.

Figure 4. a) Average perceptual scale across all subjects as a function of luminance contrast levels (black dots). b-c) Average perceptual scales for each group as a function of luminance contrast levels: joint representation for the set of groups (b); separated representation for each group (c). Michaelis-Menten function was fitted by non-linear mixed-model (dash curve). Vertical bars indicate errors with 95% confidence intervals.

Figure 5. Cerebral blood flow (CBF) measured across all subjects and for each group in the three ROIs (Superior Colliculus: SC, Lateral Geniculate Nucleus: LGN and primary visual area V1). Left and right parts of each ROI were combined. The vertical bars represent standard deviation. *$p<.01$ **$p<10^{-3}$.

Figure 6. Average variations of the BOLD signal in the ROIs (Superior Colliculus: SC, Lateral Geniculate Nucleus: LGN and primary visual area V1) according to the luminance contrast changes versus fixation for all subjects (n=30). Left and right parts of each ROI were combined. Vertical bars indicate errors with 95% confidence intervals. A.U.= Arbitrary Unit.

Figure 7. Variations of the BOLD signal in the ROIs (Superior Colliculus: SC, Lateral Geniculate Nucleus: LGN and primary visual area V1) according to the luminance contrast change vs fixation for each age group. Left and right parts of each ROI were combined. Vertical bars indicate errors with 95% confidence intervals. * $p<.05$ ** $p<.005$. A.U.= Arbitrary Unit.

Figure 8. Correlation between Age and BOLD response for Lateral Geniculate Nucleus (LGN) and primary visual area V1. Left and right parts of each ROI were combined.

Table 1. Mean cerebral blood flow expressed in mg/100ml/mn measured in the ROIs (Superior Colliculus: SC, Lateral Geniculate Nucleus: LGN and primary visual area V1) for each group. Left and right parts of each ROI were combined. sd=standard deviation.

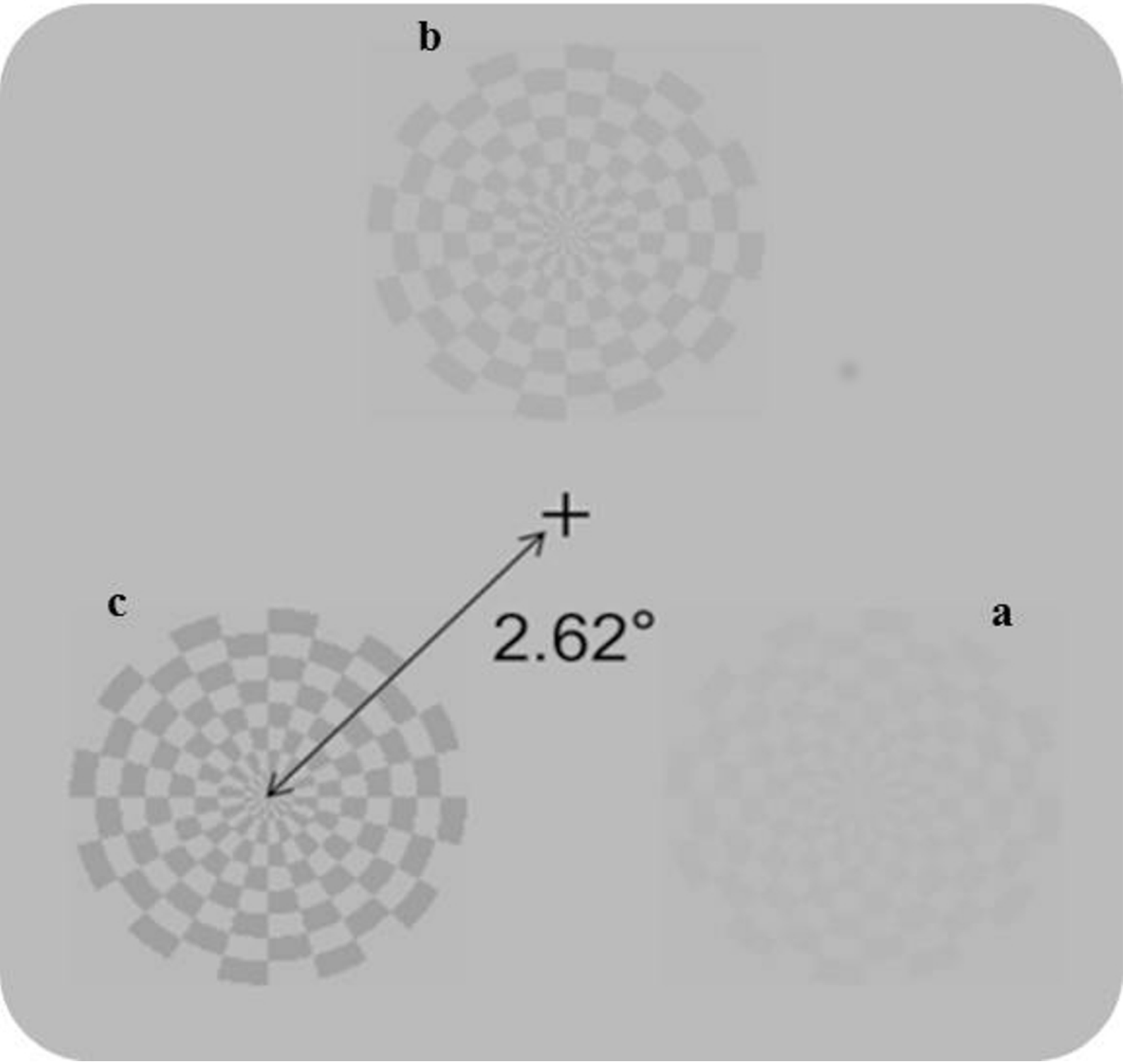
b
c
2.62°
a

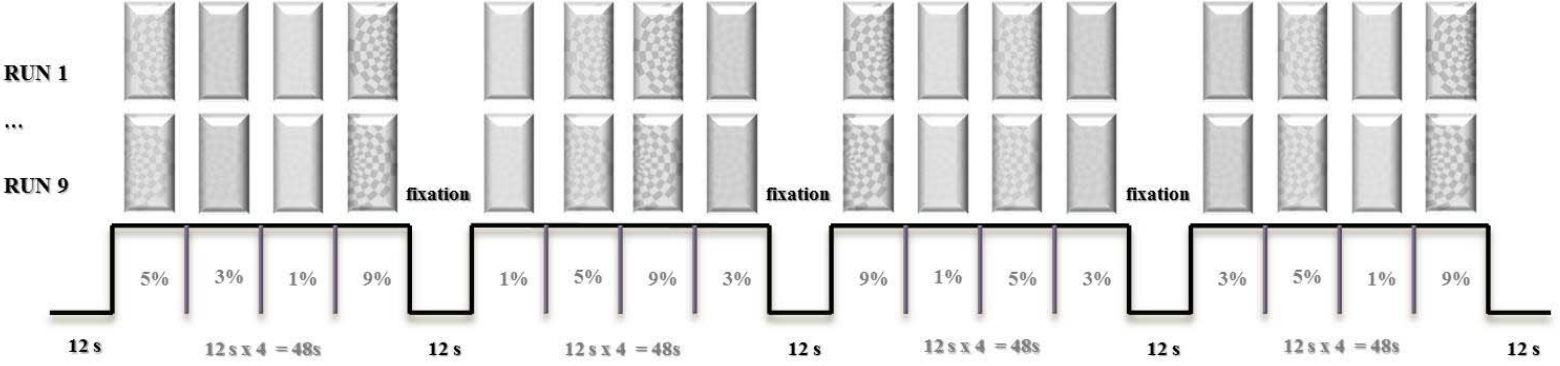
RUN 1
...
RUN 9
fixation
fixation
fixation
5%
3%
1%
9%
1%
5%
9%
3%
9%
1%
5%
3%
3%
5%
1%
9%
12 s
12 s x 4 = 48s
12 s
12 s x 4 = 48s
12 s
12 s x 4 = 48s
12 s
12 s x 4 = 48s
12 s

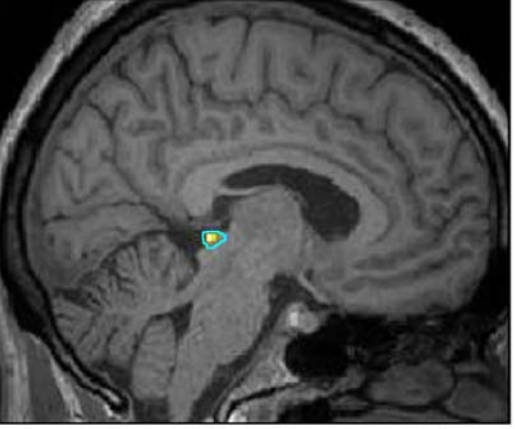

x = 6

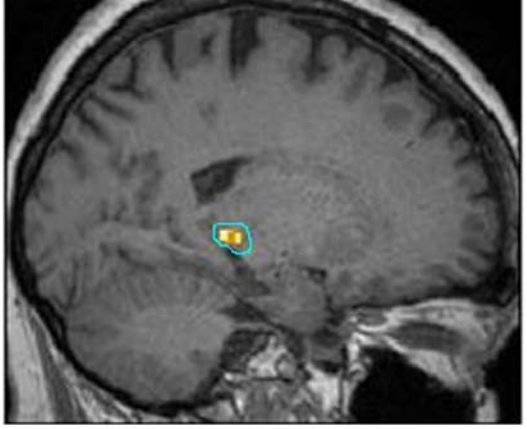

x = 23

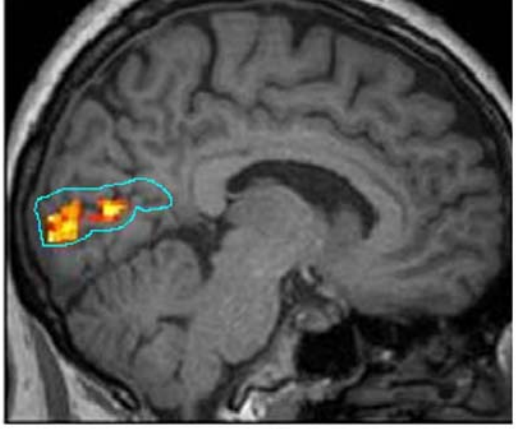

x = 8

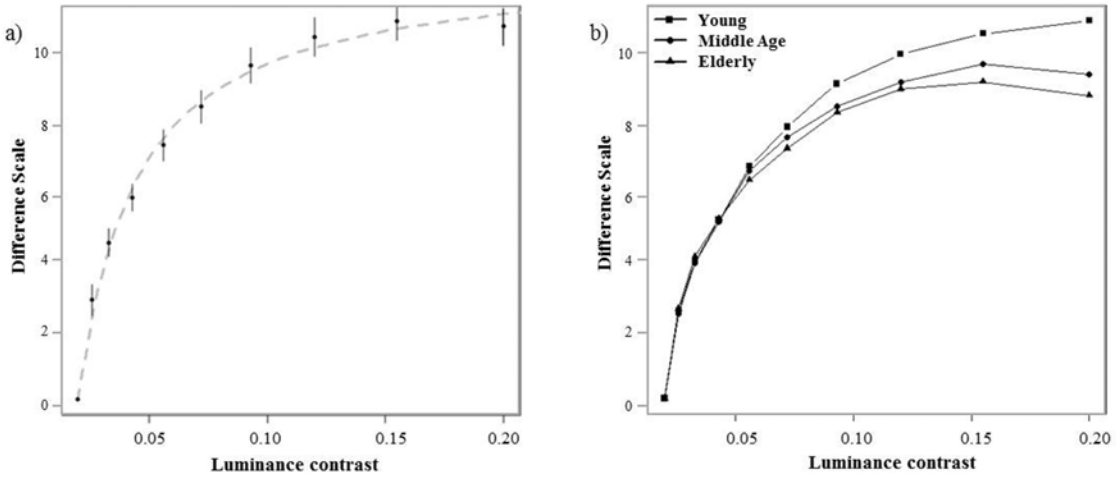
a)
Difference Scale
Luminance contrast
b)
Young
Middle Age
Elderly
Difference Scale
Luminance contrast

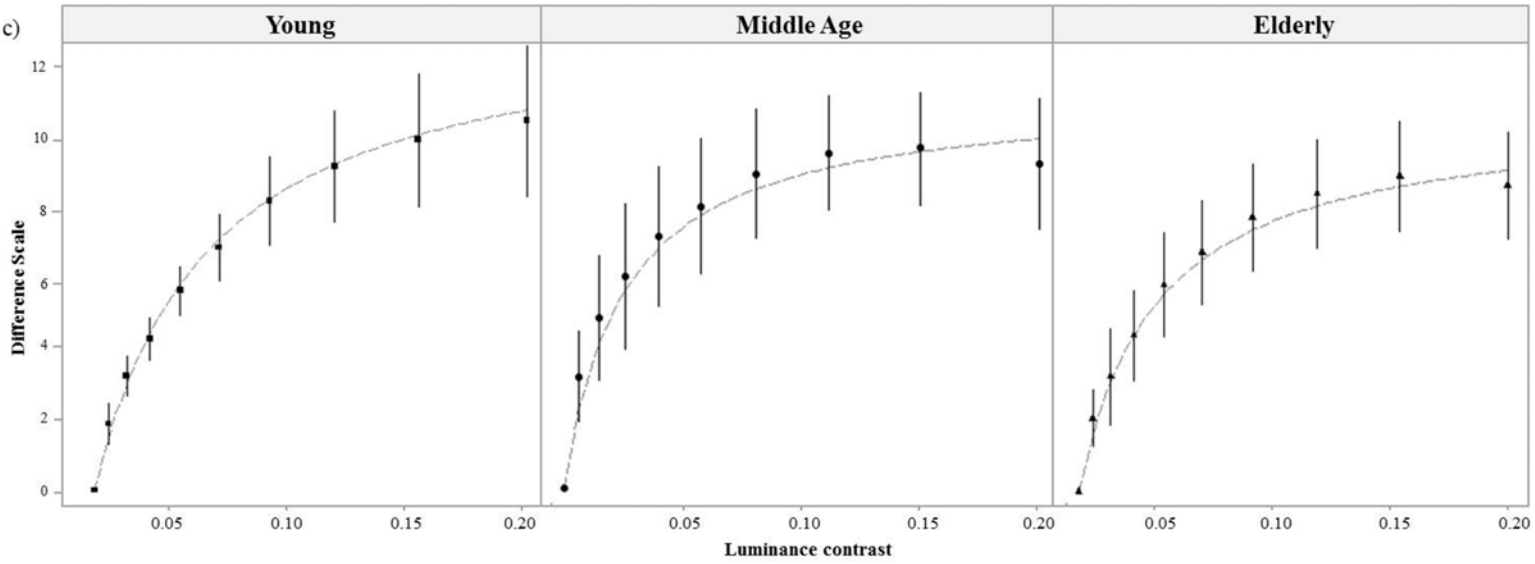
c)
Young
Middle Age
Elderly
Difference Scale
Luminance contrast

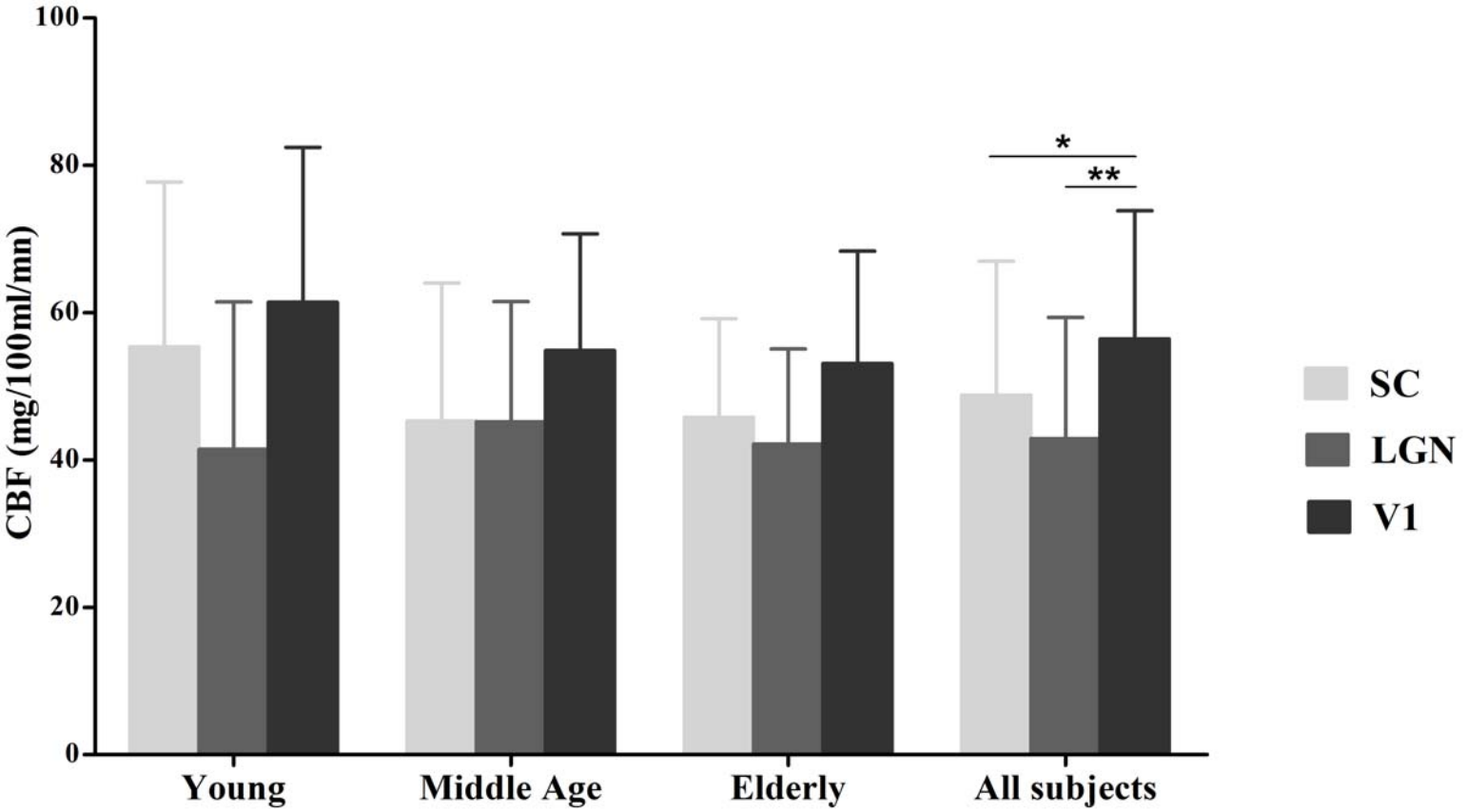
100
80
60
40
20
0
CBF (mg/100ml/mn)
*
**
SC
LGN
V1
Young
Middle Age
Elderly
All subjects

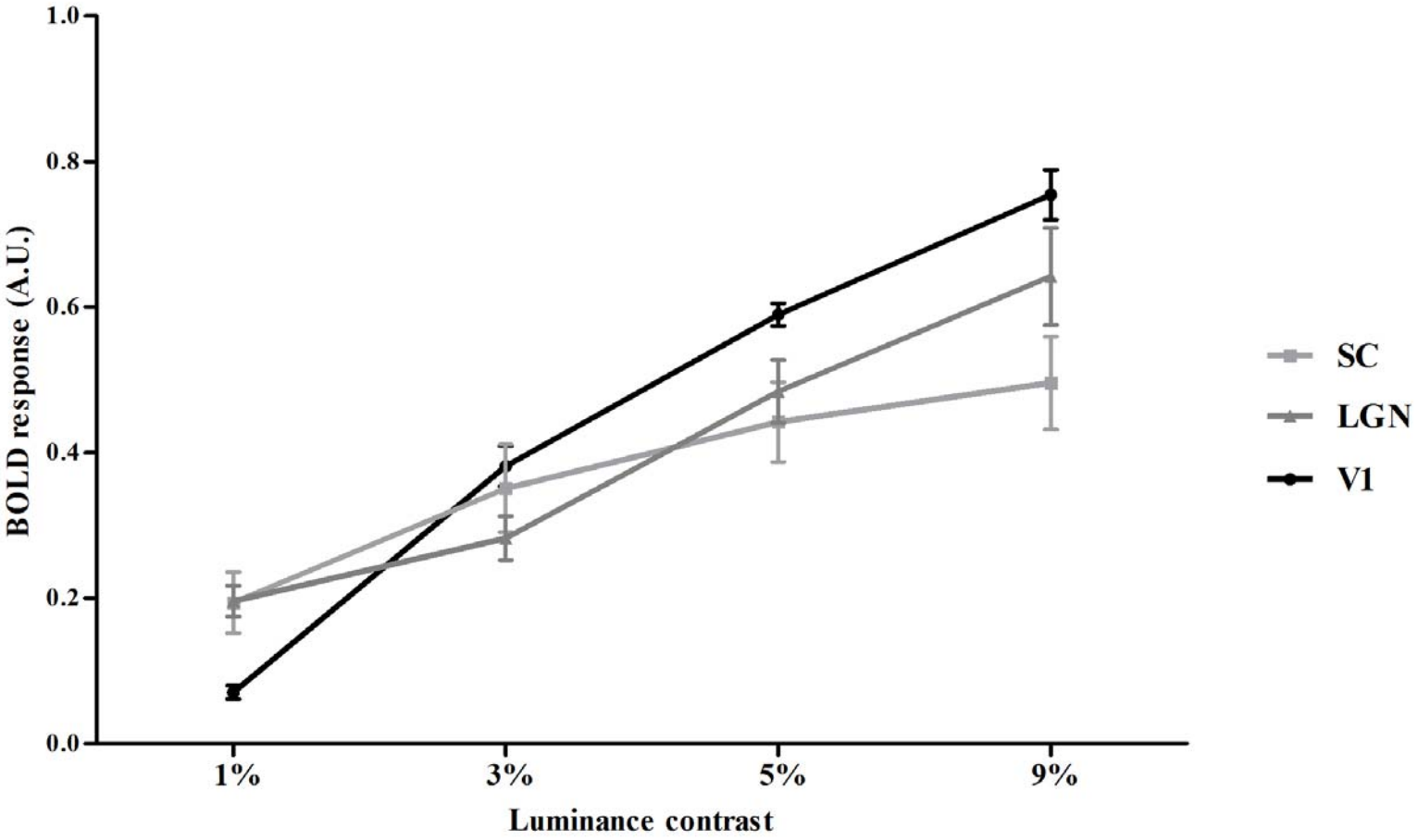
1.0
0.8
0.6
0.4
0.2
0.0
BOLD response (A.U.)
1%
3%
5%
9%
Luminance contrast
SC
LGN
V1

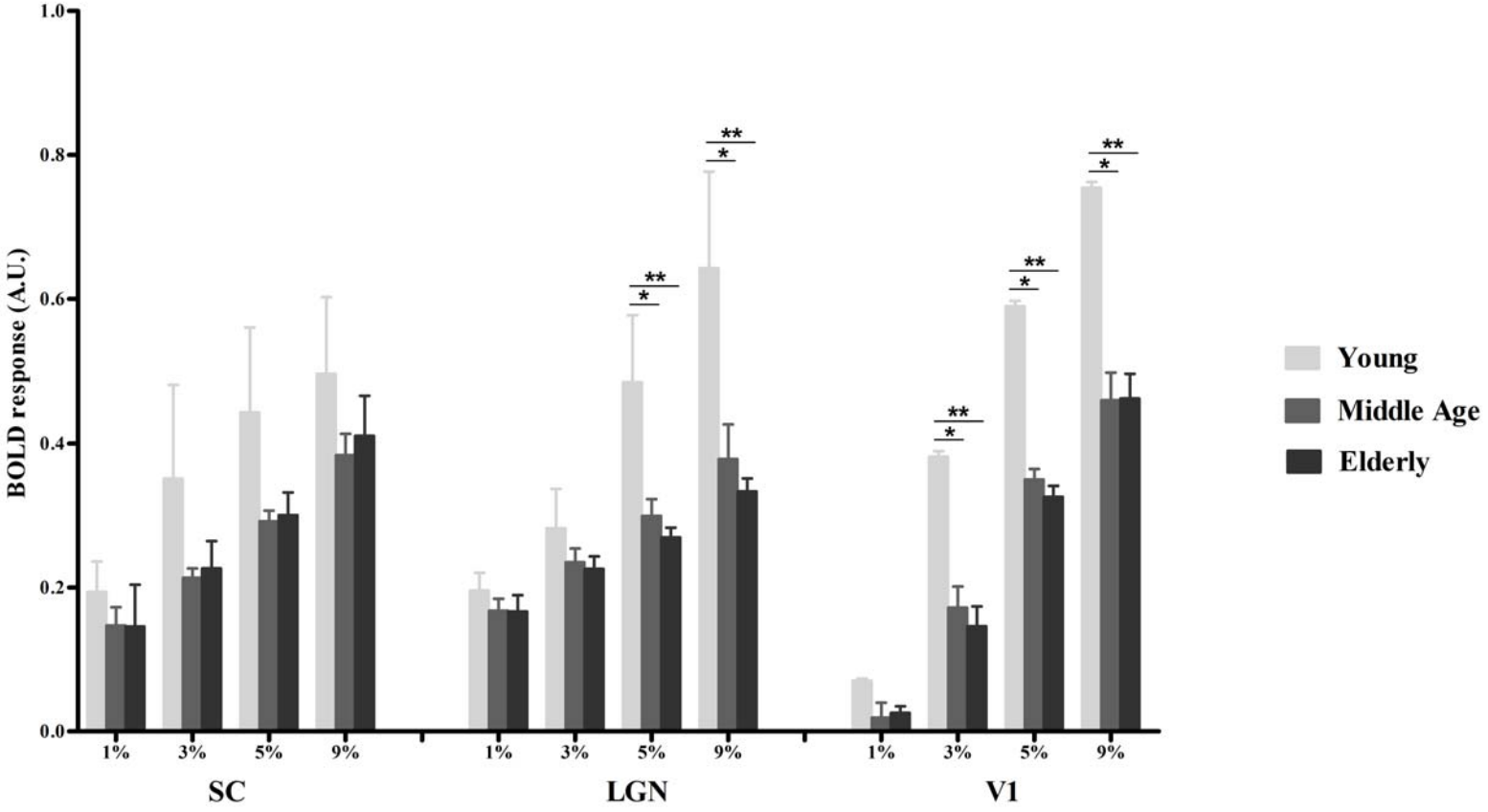
BOLD response (A.U.)
1.0
0.8
0.6
0.4
0.2
0.0
1%
3%
5%
9%
SC
LGN
V1
Young
Middle Age
Elderly
**
*

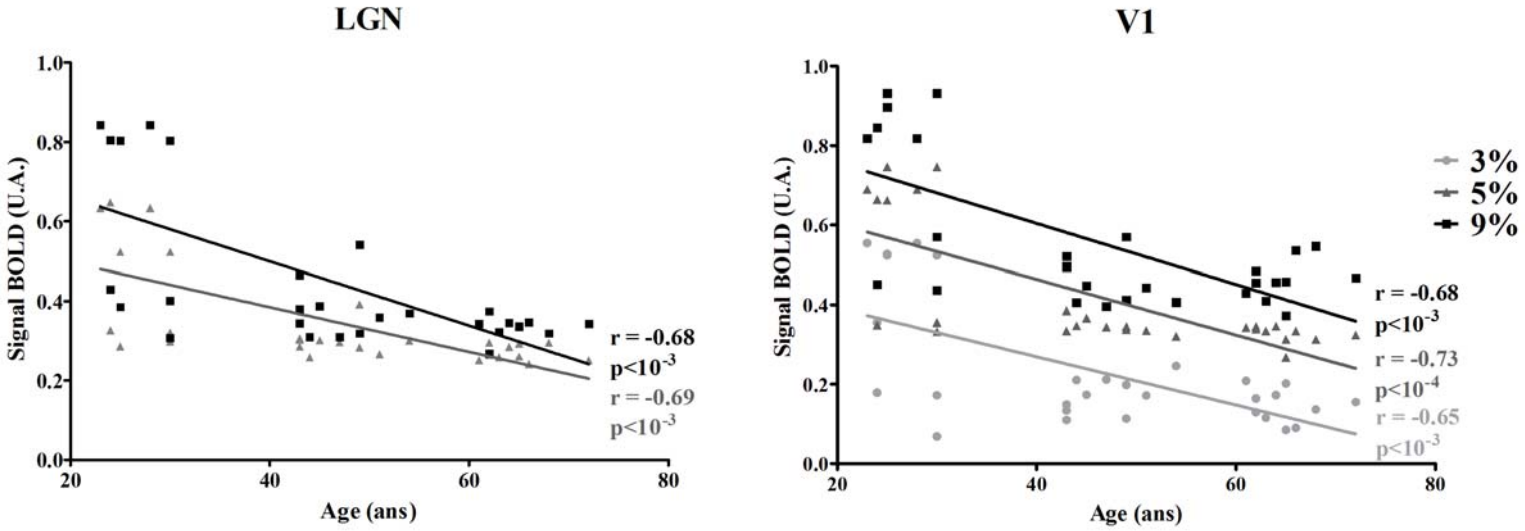
LGN
V1
Signal BOLD (U.A.)
Age (ans)
1.0
0.8
0.6
0.4
0.2
0.0
20
40
60
80
r = -0.68
p<10-3
r = -0.69
p<10-3
3%
5%
9%
r = -0.68
p<10-3
r = -0.73
p<10-4
r = -0.65
p<10-3

	SC (mean ± sd)	V1 (mean ± sd)	LGN (mean ± sd)
Young	**55.36** *± 24.92*	**61.43** *± 22.20*	**41.45** *± 21.15*
Middle age	**45.32** *± 21.96*	**54.85** *± 17.33*	**45.16** *± 18.69*
Elderly	**45.78** *± 12.45*	**53.10** *± 15.38*	**42.18** *± 12.70*